Korean J. Chem. Eng., 34(9), 2355-2365 (2017)
DOI: 10.1007/s11814-017-0199-6
pISSN: 0256-1115
eISSN: 1975-7220

INVITED REVIEW PAPER

Soft-, shape changing materials toward physicochemically powered actuators

Tae Soup Shim*,,† and Ju Min Kim*,****

*Department of Chemical Engineering, Ajou University, Suwon 16499, Korea
**Energy Systems Research, Ajou University, Suwon 16499, Korea
(*Received 29 May 2017 • accepted 13 July 2017*)

Abstract−A shape changing material (SCM) morphs its shape upon external stimulus, and it offers a design of complex 3-dimensional structures remotely, which can be potentially useful for biomedical tools, drug delivery, and soft robotics. To actuate such structures through a physicochemical stimulus, stimuli-responsive materials have been studied over the past few decades. Several SCMs have been reported by combining novel stimuli-responsive materials, micropatterning techniques and a unique actuation cue. In this review, we introduce a recent development in SCMs within the aspects of their materials and structures to describe how the materials can be designed and actuated on demand. Finally, we discuss the future direction and challenges for SCMs as physicochemically-powered actuators.

Keywords: Shape Changing Materials, Stimuli-responsive Materials, Actuators, Soft Robots

INTRODUCTION

Stimuli-responsive materials have long been studied as a novel matter in the design of physicochemically programmed tools. These are mostly made of soft matter, where the volume can be swollen or shrunk upon various environmental stimuli such as temperature, pH, electromagnetic waves, specific ions, and so on, driven by the thermodynamic equilibrium [1,2]. This diversity enables the development of stimuli-responsive materials as smart drug carriers, chemical or optical sensors as well as beneficial ingredients for foods and cosmetics. Recently, extensive studies have combined the stimuli-responsive materials with micropatterning technologies to boost the development of novel tools, so called shape changing material (SCM) [3-5]. Stimuli-responsive SCMs refer to materials that can change their structures or shapes upon stimuli. It can be easily achieved by designing composite structures with stimuli-responsive materials as an active layer and inert materials as a supporting layer. With this anisotropic design of the microstructures, an omnidirectional change in volume of the stimuli-responsive materials is hindered by the supporting layer, resulting in a directional change in volume, which enables controlled shape change of the materials. There are basically two different approaches for engineering SCMs: surface wrinkling or self-folding by introducing a solid supporting layer or a soft supporting layer, respectively. Although these structures have quite similar shape-changing strategies in their material design, these have been investigated for the use in various fields of applications.

SCMs are also called as self-scrolling, self-rolling, self-curling, or origami folding materials based on their mode of actuation and are regarded as a promising tool to design physicochemically-powered actuators. With the proper design of the materials and shapes, we can manipulate the shape changing direction, curvature or folding angle, and, eventually, its 3-dimensional shape of the material. For example, the active layer becomes the innermost or outermost layer when its volume is shrunken or swollen, respectively. The curvature of the materials is determined by the degree of change in volume of the active layer according to the dimension and mechanical properties of the materials. Thus, we can drive the material to be folded, curled, twisted, or even formed into a more complicated shape.

In this review, we introduce the recent development of soft and stimuli-responsive SCMs. In particular, we mainly focus on the material and chemical engineering aspects of the SCMs. The review is categorized into two aspects: (1) in the first section, the material aspects of SCM will be considered to introduce various stimuli-responsive systems, and then (2) the structural aspects of the materials will be discussed to introduce how the shape of material can be designed for programmable actuation. Finally, we discuss the future direction of SCMs as physicochemically-powered actuators, including some challenges in the field.

MATERIAL ASPECTS OF SHAPE CHANGING MATERIALS

1. Hydrogels

In developing SCMs, many researchers have focused on finding novel materials as an active domain. Hydrogels are the most common materials; these swell by absorbing water through a sparse polymeric network, as schematically illustrated in Fig. 1. The degree of swelling of the monolithic hydrogel can be tuned according to the crosslinking density, polymerization yield, and molecular structure of the materials. Therefore, SCMs can be simply realized by combining swellable hydrogels with non-swellable supporting materials (Fig. 2(a)). Interestingly, a similar bilayer type of structure, such as bimetallic strips, has been previously utilized for thermosets, clocks, electrical devices, and so on. In addition, this mechanism is

†To whom correspondence should be addressed.
E-mail: tsshim@ajou.ac.kr

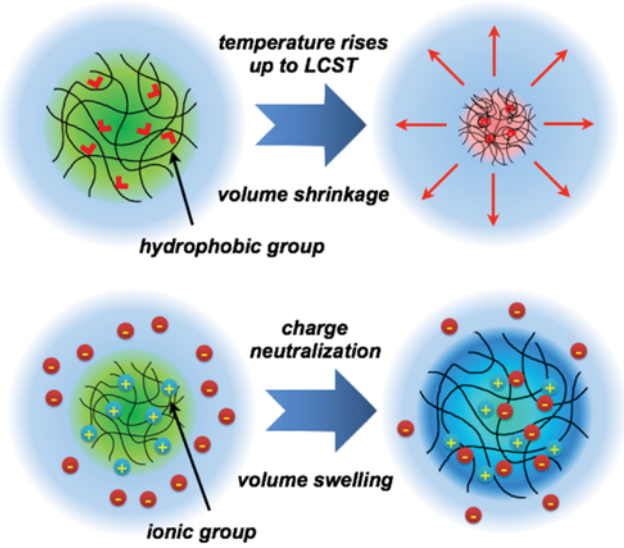

Fig. 1. Schematic illustration of reversible swelling/shrinkage of hydrogels response to temperature (top) and pH (bottom).

also frequently observed in nature [6,7]. The deposition of a metal thin film on a hydrogel film can realize self-bending. Since the hydration of the hydrogel exerts strain onto the film, the hydrogel/metal composites show reversible bending. For example, Ma *et al.* mimic a humido-sensitive blooming of a flower's petals by fabricating swellable poly(acrylic acid) (PAA)/poly(allyl-amine hydrochloride) (PAH) layer-aluminum bilayer, as shown in Fig. 2(b) [8]. By controlling the degree of hydration [9] or crosslinking the density of the materials [10], the same strain can be applied onto materials, which may result in a different curvature of the bent structures. In the same manner, a more complicated swelling-driven shape change can be achieved by applying micropatterning technology, which will be discussed later.

The great strength of hydrogels as an SCM is their capability to achieve a dramatic change in volume upon an external stimuli. The first temperature-responsive self-folding material (Fig. 2(c)) was reported in 1995 by Hu et al. [11], and since then, poly(N-isopropylacrylamide) (PNIPAM) has become a representative material to fabricate stimuli-responsive SCMs. PNIPAM is a polymer that has a lower critical solution temperature (LCST) near human body temperature, reversibly changing its phase between the hydrated state and dehydrate state. The volume of dehydrated PNIPAM is known to be approximately 10% compared to that of its hydrated state, which is enough of a deformation for self-folding. In fact, most SCMs have used PNIPAM- or PNIPAM-based composite materials as a backbone since these are easy to fabricate and actuate in relatively moderate environmental conditions. The high volumetric shrinkage of PNIPAM enables transformation of planar bilayer films into tubular structures. The Ionov group fabricated PNIPAM-based bilayer films with a very low aspect ratio to achieve rolling of the film to encapsulate the microspheres, as shown in Fig. 2(d) [12]. In addition, the dimension of the film is also controlled using photolithography, which realizes long-side, short-side, or diagonal curling of materials showing programmable actuation [13].

As a stimulus, light is a powerful tool since it enables the remote and spatial control of actuation. Temperature-responsive hydrogels can also be light-responsive since light generates heat by additives, as shown in Fig. 2(e). Since light can be spatially and temporally controlled, the shape change of the PNIPAM bilayer film can be achieved with a greater degree of freedom. As shown in Fig. 2(f) and 2(g), reprogrammable SCMs are demonstrated by incorporating gold nanoparticles [14] or magnetic nanoparticles [15,16] into PNIPAM hydrogels. The photothermal effect with nanoparticles enables local heating of materials and enhances the actuation kinetics of SCMs. In addition, Fig. 2(h) shows that the degree of swelling is also controlled by manipulating the light intensity, remotely, showing a facile way to control the SCMs. Recently, graphene oxide was used for its photothermal effect on SCMs showing sunlight driven actuation [17].

Another frequently used hydrogel is the one with pH-responsiveness. The pH-responsive swelling behavior of the hydrogel has been previously well established [18]. When the backbone of the hydrogel network has either cationic or anionic groups upon hydration, the charge neutralization process within the hydrogel network derives swelling of polymer network. Specifically, the hydrogel with a cationic group, such as an amide, or anionic group, such as a carboxylate, swells more in acidic or basic condition, respectively, since these absorb counterions, as shown in Fig. 2(i). Using these characteristics, various hydrogels have been designed as pH-responsive materials. For example, biocompatible hydrogels made of poly(2-hydroxyethylmethacylate), (p(HEMA)) are copolymerized with acrylic acid (AA) (p(HEMA-*co*-AA)) for base-swellable hydrogels [19]. Then, these are fabricated with p(HEMA) as a bilayer using two-step photolithography. The proper design of a planar bilayer film offers the transformation of the film into 3-dimensional microcapsules in a basic solution (Fig. 2(j)). A similar active layer composed of p(HEMA-*co*-AA) with poly(ethylene glycol) diacrylate (PEGDA) and a supporting layer of poly(divinylbenzene) shows reversible bending with a pH condition [20]. The curvature attributed to the self-folding of the bilayer film is controlled by thickness of the supporting layer due to the force balance between the tensile force of the active layer and the material stiffness of the supporting layer. On the other hand, the hydrogel with the amine group swells in an acidic condition. PNIPAM, a thermo-responsive hydrogel, can also be used as an acid-swellable hydrogel due to its acrylamide group shown in Fig. 2(k) [21]. As far as biomedical applications are concerned, SCMs made of fully biocompatible and biodegradable materials is practically important; among natural polysaccharides, chitosan is a good example with an amine group. To achieve this, SCMs fully designed with natural polysaccharides, chitosan and cellulose/carboxymethylcellulose, are used for the actuation [22].

Some hydrogels are actuated with unconventional responses. Maeda et al. used a unique chemical reaction, called the Belousov-Zhabotinsky (BZ) reaction inside of PNIPAM gels for the periodic actuation of hydrogels [23]. The BZ reaction catalyst, ruthenium(II) tris(2,2′-bipyridine) ($Ru(bpy)_3^{2+}$), is covalently bonded with PNIPAM, and the molecular state of the catalyst is reversibly changed from an oxidized Ru(III) state to a reduced Ru(II) state. As a result, the chemical waves drive a cyclic oscillation of the hydrogels, as

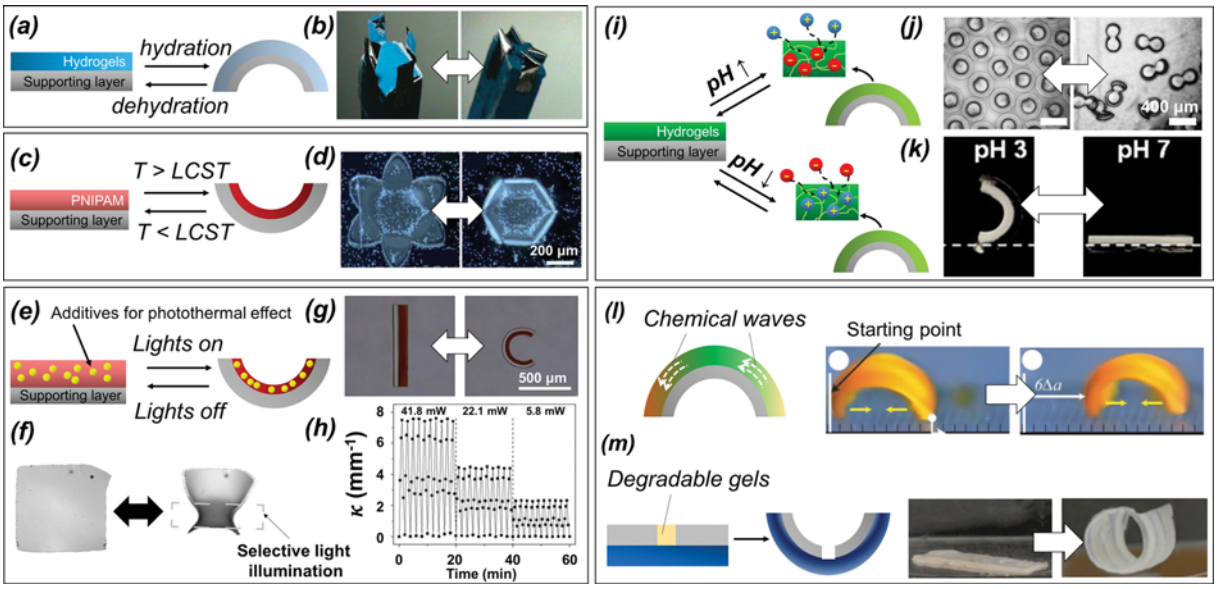

Fig. 2. (a) Schematic illustration of shape changing material (SCM) made of stimuli-responsive hydrogels that can be actuated by hydration. (b) Images of free standing aluminum and 30 layers of poly(acrylic acid)/poly (allylamine hydrochloride) bilayers at 12% relative humidity (RH) (left) and 5% RH (right) at 60 °C showing shape changing upon hydration. Reproduced with permission [8]. Copyright 2009, American Chemical Society. (c) Schematics of temperature-responsive actuation of hydrogels. (d) Images showing temperature-responsive actuation of poly(N-isopropylacrylamide)-co-poly(4-acryloylbenzophenone) (PNIPAM-ABP) and polycaprolactone bilayer for capturing yeast cells at below lower critical solution temperature. Reproduced with permission [11]. Copyright 2011, The Royal Society of Chemistry. (e) Schematics of photothermally-triggered actuation of hydrogels. (f) Images of PNIPAM gels with gold nanoparticles. As the light is selectively illuminated, surface plasmon resonance absorption of gold nanoparticle generate heat resulting deswelling PNIPAM gels. Reproduced with permission [14]. Copyright 2014, Wiley-VCH. (g) Photothermal actuation of PAAm and PNIPAM/magnetic nanoparticle bilayers under visible light. Light absorption of magnetic nanoparticles make deswelling of PNIPAM layer. (h) A graph for reversible and controllable actuation of bilayer film. In accordance with light intensity, curvature (κ) of film is consistently controlled. Panel (g), (h) are reproduced with permission [16]. Copyright 2015, Nature Publishing Group. (i) Schematics of pH-responsive actuation of hydrogels. Negatively or positively charged hydrogels are swells at alkalic or acidic conditions, respectively. (j) Images for reversible folding of poly(hydroxyethylmethacrylate) and poly(hydroxyethylmethacrylate-co-acrylic acid) bilyer film by pH. The planar film forms microcapsules at alkalic solution of pH 9 (left) and recovers its flat shape at acidic condition of pH 4 (right). Reproduced with permission [19]. Copyright 2012, Wiley-VCH. (k) Acid-responsive folding of poly(N-isopropylacrylamide-co-2-carboxyisopropylacrylamide) and poly(N-isopropylacrylamide-co-N,N′-dimethylaminopropylacylamide) bilayer. A layer containing carboxyisopropylacrylamide units swells at acidic solution, resulting bending of materials. Reproduced with permission [21]. Copyright 2012, The Royal Society of Chemistry. (l) Schematics of periodic chemical reaction-driven actuation (left) and images of self-walking motion of poly(NIPAM-co-ruthenium(II) tris(2,2′-bipyridine)-co-2-acrylamide-2-methylpropane sulfonic acid) gels on ratcheted substrate (right). By the Belouzov-Zhabotinsky reaction, state of ruthenium changes from oxidized to reduced state periodically, resulting autonomous swelling/deswelling of gels. Produced with permission [23]. Copyright 2007, Wiley-VCH. (m) Schematics of strain-triggered actuation of SCMs by degradation of hydrogels (left) and images for curling of poly(ethylene glycol) diacrylate, gelatin methacrylate-co-polyethylene glycol dimethacrylate (GelMA-co-PEGDMA), and PNIPAM hybrid gels. Enzymatic degradation of GelMA causes decrease of crosslinking density of GelMA-co-PEGDMA layer resulting film curling. Reproduced with permission [25]. Copyright 2016, American Chemical Society.

shown in Fig. 2(l). The degradation of the gel with a biological signal induces a change in the shape of the hydrogels [24,25]. Athas et al. harnessed gelatin methacrylate as a degradable layer by collagenase [25]. They fabricated PNIPAM and an alternating PEGDA-gelatin methacrylate bilayer film. As the gelatin methacrylate layer becomes degraded by the collagenase, as shown in Fig. 2(m), the swelling force of the PNIPAM layer makes a change in the shape of the materials.

Most hydrogel-based SCMs are actuated in a hydrated state. Also, many actuation cues are closely related to the biological conditions. The temperature-responsive hydrogels respond to body temperature, and the pH-responsive hydrogels can be potentially used as actuators in specific organs with different pH conditions. Recent developments have shown that biological signals can trigger the actuation of the materials, and these results imply the future applicability of hydrogel-based SCMs as a soft robot in the human body.

2. Shape Memory Polymers

Shape memory polymers can memorize the shape or mechanical state, and these have the ability to recover their shape from a deformed state to a permanent state, which offers programmability as SCMs [26-30]. Unlike the hydrogel based on the SCM, which always requires a wet environment, the shape memory polymer can be actuated in both dry and wet states. A common shape memory polymer is controlled by the temperature. From its permanent shape, it can be deformed into various shapes by elevating

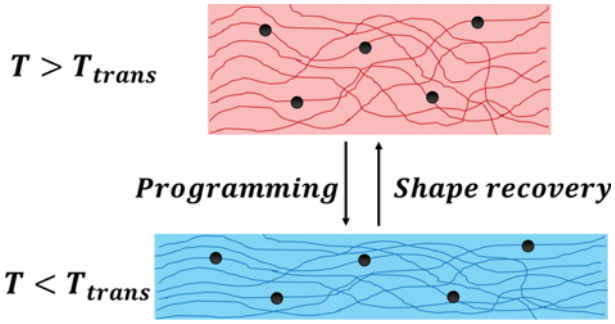

Fig. 3. Schematic illustration of shape recovery of shape memory polymer. Shape of polymer is programmed above thermal transition temperature (T_{trans}), then cooled for shape fixation. The shape can be recovered as we increase the temperature to T_{trans}.

the temperature to the thermal transition temperature (T_{trans}) of the materials. The deformed shape is maintained below T_{trans}, but it readily recovers its shape when we increase the temperature to T_{trans}, as shown in Fig. 3. By using this characteristic, the commercially-available shape memory polymer, Shrinky-Dinks, is used as an SCM [27]. For photothermally triggered shape changes, light absorption ink patterned on Shrinky-Dinks enables a programmed deformation of the planar film when it is illuminated with infrared light. Since the deformation of the film occurs only at a temperature above T_{trans}, the structure becomes bistable at room temperature. A similar approach has also incorporated nanoparticles into the shape memory polymers (Fig. 4(a)). Zhang et al. demonstrated light-driven SCMs by using the photothermal effect of gold nanoparticles [28,29]. Interestingly, the gold nanorods in the shape memory polymer were shown to be aligned by polarized light because of the anisotropic optical property of the gold nanorods. They incorporated gold nanorods in poly(vinyl alcohol) film, and then it was stretched to align the gold nanoparticles. In these states, the deformed stretched film can be initially recovered to the stretched state through parallel polarized light, as shown in Fig. 4(b). Although the above examples only achieve irreversible actuation, it shows the potential to use light as the actuation cue to control the shape memory polymers.

The general shape of the shape memory polymer has limitations for engineering: 1) the deformation process is irreversible, and 2) a permanent shape cannot be redefined. To overcome these limitations, the shape memory polymer with a crystallizing domain was introduced to produce bi-directional reversible SCMs [31,32]. Briefly, reversible-shape memory polymers can be realized utilizing multiple transition points, as shown in Fig. 4(c). Since the shape of the polymer is programmed by heating over the glass transition temperature (state I) followed by a cooling (state II), the crystalline domains in the material can reversibly change its state upon moderate heating (state III) and cooling. These multiple states are designed through the copolymerization of materials. As shown in Fig. 4(d), the multiphase polymers consisting of poly(ω-pentadecalactone) segments acting as the geometry-determining domains

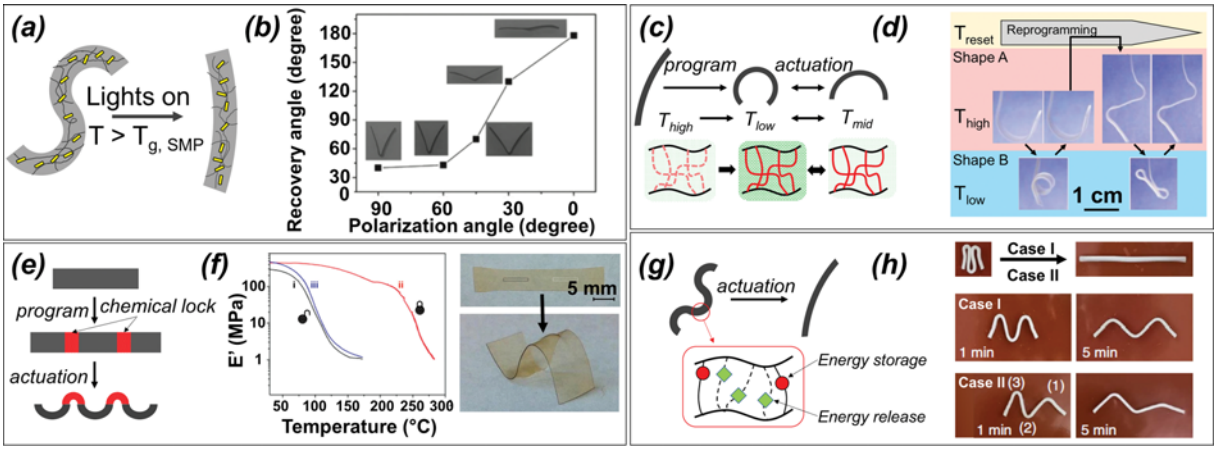

Fig. 4. (a) Schematic of shape recovery of shape memory polymer by photothermal effect. (b) A graph for polarization angle dependent shape recovery of poly(vinyl alcohol) film incorporated with gold nanorods. Since photothermal effect of gold nanorods is maximized when the light polarization is parallel to the direction of gold nanorods, shape recovery is effected by polarization angle of light. Reproduced with permission [28]. Copyright 2013, Wiley-VCH. (c) Schematic of reversible actuation of shape memory polymer having multiple equilibrium states. (d) Images of reprogramming and reversible actuation of poly(ω-pentadecalactone)/poly(ε-caprolactone) composite film. The film is programmed above geometry determining temperature, T_{reset}, and is actuated at actuation temperature, T_{high} by controlling crystallization of each polymer domains. Reproduced with permission [31]. Copyright 2013, Wiley-VCH. (e) Schematic of actuation of chemically-programmed shape memory polymers. (f) Dynamic mechanical analysis for thermal relaxation of Nafion film at deprotonated (red) and re-protonated (blue) states (left). When the film is immersed in 1 M NaOH (deprotonation) and 1 M HCl (re-protonation), thermal relaxation temperature is around 260 °C and 100 °C, respectively. Selective deprotonation of Nafion film show programmed shape changing at 120 °C (right). Reproduced with permission [33]. Copyright 2014, Wiley-VCH. (g) Schematic of temporally controllable shape memory polymer having dual networks. (h) Two different cases for actuation of N,N-dimethylacrylamide-co-methacrylic acid polymers, with different shape recovery paths. Case I is programmed identically while relaxation time for three kinks in case II is programmed for different timescale resulting sequential actuation. Reproduced with permission [35]. Copyright 2016, Nature Publishing Group.

and poly(ε-caprolactone) segments providing actuator domains, display programmable and reversible shape changes [31]. Multi-

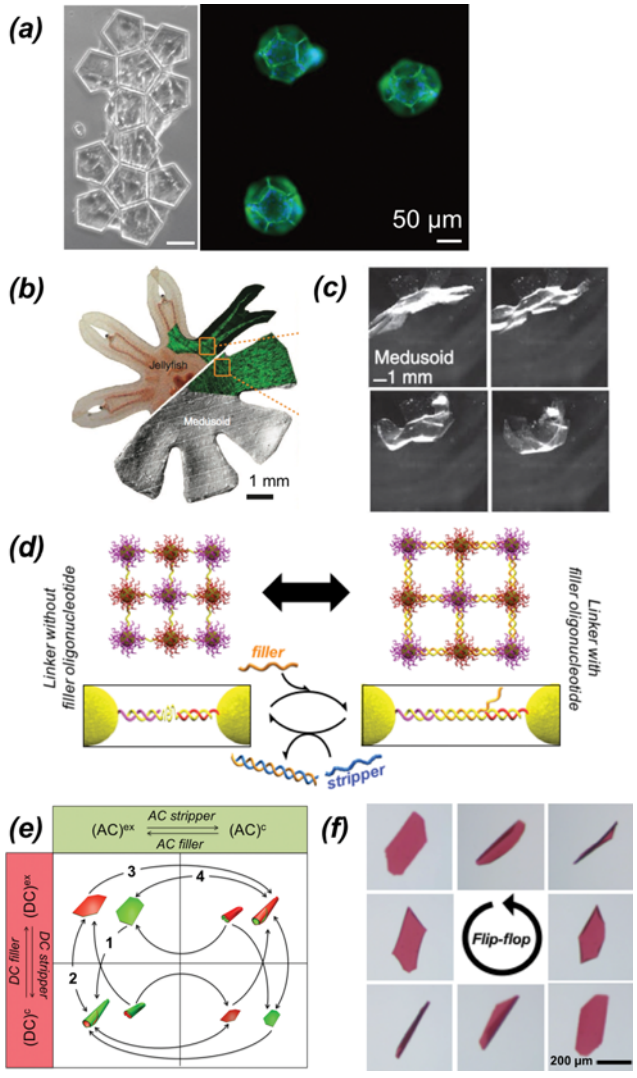

Fig. 5. (a) Optical (left) and confocal microscope (right) images of NIH/3T3 cell covered dodecahedron microplate before (left) and after (right) folding by cell traction forces. Reproduced with permission [36]. Copyright 2012, Public Library of Science. (b) Graphics for cross-section of jellyfish (top) and jellyfish mimic SCMs made of poly(dimethylsiloxane) with muscle tissues. (c) Movie snapshots for jellyfish-like movements by applying 1 Hz, 2.5 V cm^{-1} of alternating current electric field. The pace of actuation follows frequency of electric field. Panel (b), (c) is reproduced with permission [37]. Copyright 2012, Nature Publishing Group. (d) Design for expansion and contraction of DNA structures by reversible hybridization. Single strand gap (yellow) between DNA-gold nanoparticles forms duplex by filler DNA (orange) and the filler DNA can be removed by stripper DNA (blue) followed by thermodynamic equilibrium. (e) Actuation routes of dual addressable DNA-gold nanoparticle bilayer film where each domain is programmed with different DNA sequences. (f) Movie snapshots for programmed flop-flop actuation followed by actuation routes in (e). Panel (d)-(f) is reproduced with permission [38]. Copyright 2017, Nature Publishing Group.

programming of the shape memory polymer can also be achieved by fixing the shape via chemical patterning (Fig. 4(e)) [33,34]. For example, Kohlmeyer et al. used chemical locking of Nafion with reversible deprotonation upon a change in the pH in the solution to encode, erase, and re-encode the shape information of materials, which makes the shape memory polymers have a high complexity upon shape programming (Fig. 4(f)). One interesting shape memory polymer that can program the time of actuation was recently reported [35]. It is realized by designing dual polymer networks: chemical networks between N,N-dimethylacrylamide and methacrylic acid for energy storage and physical networks of hydrogen bonding for controlled energy release, as shown in Fig. 4(g). Note that rearranging the hydrogen bonding only contributes to the kinetics of the shape recovery, maintaining the shape deformation of the materials (Fig. 4(h)).

3. Specially Designed Materials

Beyond the materials described above, there are specially designed materials with unique actuation cues. The cells naturally pull each other through actomyosin interactions and actin polymerization, generating a cell traction force. Kuribayashi-Shigetomi et al. combined a patterned polymer substrate and cell traction force to generate 3-dimensional structures (Fig. 5(a)) [36]. The muscular cells' kinetic movements with an electric signal can be used directly for a jellyfish-like shape change as shown in Fig. 5(b). By aligning the muscular tissues on the elastic polymer substrate mimicking the jellyfish's muscles, the biomimetic propulsion of the polymeric thin film is demonstrated by applying an alternating current field [37]. The electric-field assisted propulsion of a jellyfish-like film in Fig. 5(c) suggests the utilization of multiple cells for engineering environment-sensitive SCMs.

One of the biggest issues for the design of the SCM is to develop an orthogonal stimulus for multi-responsive and programmable actuation. Although the aforementioned stimuli, such as the temperature, pH, electric field, and light have shown well-controlled actuation, designing SCMs composed of multiple active layers is challenging since the independent actuation of an active layer using different stimulus is difficult. To address this problem, the sequence-specific hybridization of the oligonucleotides can be engineered for SCMs by tuning a pre-designed molecular structure of the oligonucleotides. In particular, the structures of the single-stranded and double-stranded oligonucleotides have different molecular lengths per bases as the double-stranded oligonucleotides form helical structures. Based on this, the reversible hybridization of the oligonucleotides is applied to design the SCMs, as illustrated in Fig. 5(d). The multilayer DNA films curl in various ways by controlling the structure of the oligonucleotides [38]. Since the independent actuation of the DNA film is possible, various actuation routes have been discovered (Fig. 5(e)), which enables the robotic actuation of the structures showing flip-flop actuation (Fig. 5(f)).

STRUCTURAL ASPECTS OF THE SHAPE CHANGING MATERIALS

1. Homogeneous Bilayer Films

The SCM can be used to fabricate complex 3-dimensional structures out of 2-dimensional planar films. The lithographically pat-

terned 2-dimensional films become blueprints for 3-dimensional structures by considering the final shape. As described above, a basic way to designing the SCMs is to use two materials with different physical properties. Simple bilayer structure can be prepared by superimposing two different homogeneous thin films. Then, the change in shape is caused by the difference in the volume changing ratio between the layers. Therefore, the final shape of the film is determined by the dimension of the initial shapes. For example, the rectangular film curls in either long-side, short-side or diagonal-side in accordance with the thickness, width-to-length ratio, and initial site of curling (Fig. 6(a)). When the active layer starts expansion or shrinking, curling occurs preferentially from the periphery of the film. For the rectangular film with a high width-to-length ratio, therefore, long-side curling happens since it is energetically favorable. On the other hand, diagonal curling occurs when the width-to-length ratio of the film is close to unity, since curling is preferentially initiated from the corners of the film (Fig. 6(b)) [13]. The dimension of the film also affects the degree and kinetics of curling [20,39]. The thickness of the layers determines the torque generated by the active layer and stiffness of the film. Therefore, the degree of curling varies in a manner that is inversely proportional to the thickness of the film, as shown in Fig. 6(c). In the same manner, the speed of actuation can be enhanced as the supporting layer becomes thinner. Recently, the direction and speed of the film curling have been also controlled by punching anisotropic holes in the bilayer films [40].

2. Gradient Films

The monolithic film with the gradient micro/nanostructures shows a gradual volume expansion or shrinkage. One example of the gradient film is to use a nanoparticle-dispersed prepolymer solution (Fig. 6(d)) [41-43]. The PNIPAM-silica composite hydrogels having a domain with concentration gradient of silica nanoparticles are prepared through the electrophoresis of silica nanoparticles [41]. Negatively-charged silica nanoparticles concentrated on one

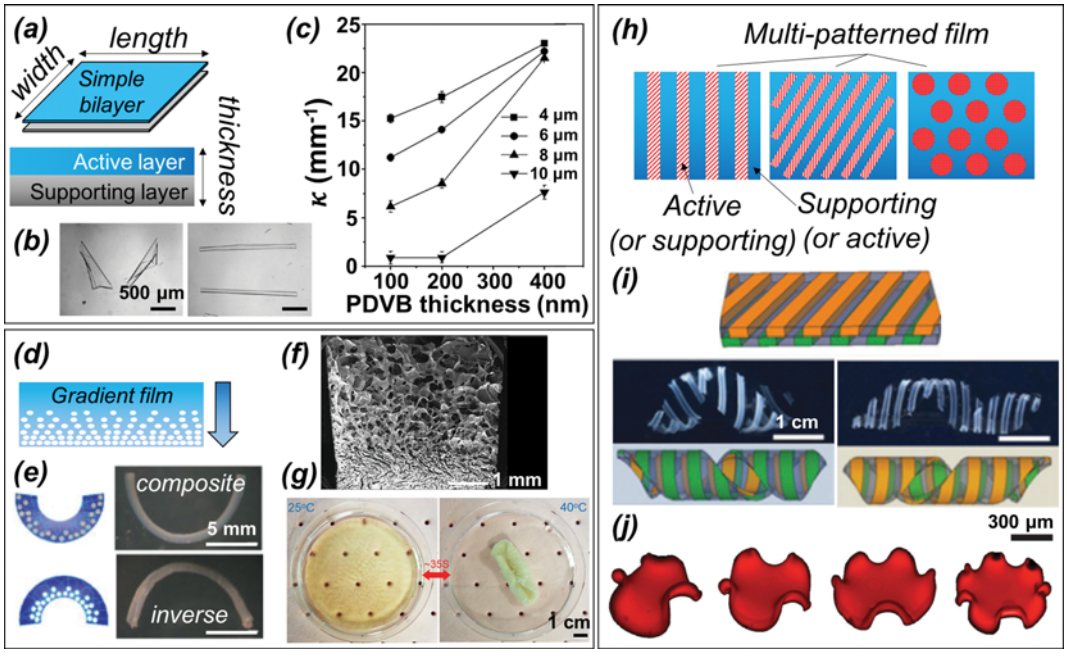

Fig. 6. (a) Schematic of a simple bilayer structure with active and passive layer. Shaping factors are width, length and thickness of film. (b) Images of curled simple bilayers of poly(NIPAM-co-benzophenone acrylate) and poly-(methylmethacrylate-co-benzophenone acrylate). Direction of curling is determined by dimension of film; long-side curling for 1,800 μm×300 μm film and diagonal-side curling for 1,000 μm×500 μm film. Reproduced with permission [13]. Copyright 2012, American Chemical Society. (c) Thickness-dependent bending curvature of poly(hydroxyethyl methacrylate)/poly(divinylbenzene) bilayer. Legends indicate thickness of active layer, poly(hydroxyethyl methacrylate), and abscissa indicates thickness of supporting layer, poly(divinylbenzene). Reproduced with permission [20]. Copyright 2016, American Chemical Society. (d) Schematics of SCM with gradient structures. In this structure, the gradient can be crosslinking density, porosity, or composition of materials. (e) Illustration (left) and images (right) of gradient hydrogels made of PNIPAM. Silica-PNIPAM composites (top) and silica removed porous PNIPAM materials (bottom) bend at 40 °C in opposite directions. Reproduced with permission [41]. Copyright 2008, Wiley-VCH. (f) Scanning electron microscope image of hydrothermally synthesized PNIPAM with gradient porosity over cross-section. (g) Images of temperature-responsive curling of gradient porous PNIPAM film with highly porous side inside. Panel (f), (g) are reproduced with permission [43]. Copyright 2015, Wiley-VCH. (h) Schematics of heterogeneously patterned SCMs. Active and supporting layers can be patterned on supporting and active layers, respectively, for advanced actuation. (i) Shape changing of heterogeneously patterned film made of poly(acrylic acid) (green), poly(1-vinylimidazole-coacrylamide) (orange),and PNIPAM (gray). The film is curled with right-handed helix (left) in pH 9 poly(acrylic acid) swells and with left-handed helix (right) in pH 1 as poly(1-vinylimidazole-coacrylamide) swells showing multiple shape changes. Reproduced with permission [48]. Copyright 2016, The Royal Society of Chemistry. (j) Confocal microscope image of PNIPAM film with axisymmetric swelling patterns. Crosslinking density of PNIPAM is spatially controlled by grayscale photomask. Reproduced with permission [54]. Copyright 2016, The Royal Society of Chemistry.

side of the PNIPAM film result in the other side of film becoming stiffer, thereby causing a gradient volume shrinkage of the PNIPAM film through an increase in temperature. After removing the silica nanoparticles using hydrofluoric acids, the silica-embedded side becomes porous, reversing the direction of bending (Fig. 6(e)). Luo et al., prepared gradient porous PNIPAM hydrogels directly through hydrothermal polymerization [43]. As the polymerization proceeds, the PNIPAM chains with hydroxyl groups precipitate, forming gradient-crosslinked structures (Fig. 6(f)). The shape changing behaviors are affected by the porosity of the films (Fig. 6(g)) in the same manner with the gradient film that was previously described.

3. Heterogeneously Patterned Films

In a similar manner as with the bilayer structures, the chemically- or physically heterogeneous film transforms into various shapes, triggered by external stimuli. The photolithography of two different polymers can generate heterogeneous structures, as shown in in Fig. 6(h). The strength of using a heterogeneous film is its higher degree of freedom of programmability. By conducting multiple micropatterning processes in series, the heterogeneous film can be folded, curled, twisted or shaped with various curvatures into one mechanical state [25,33,44-52]. For instance, the rectangular film curls in a long-side, short-side and diagonal side, followed by the direction of the alternating active domains. Controlling the direction of bending for individual layers offers various possibilities to change the shape. Such strategies can be used to realize helical structures by integrating two heterogeneous films. Wang et al. prepared two diagonally patterned films made of PAA/PNIPAM using photolithography [48]. Then, two identical patterns are assembled face-to-face making orthogonally aligned PAA/PNIPAM domains. Since two layers bend in opposite directions, the film forms a saddle-like configuration, resulting in helical structures (Fig. 6(i)). The diagonally-patterned active layers respond to different external stimuli and can be multi-responsive, which shows the numbers of different mechanical states on the actuation [47].

The heterogeneous film can be prepared not only by using different materials, but also by spatially controlling the crosslinking density of the active polymer [53-55]. Kim et al. fabricated a heterogeneous PNIPAM film by controlling the UV dose during photopolymerization. The crosslinking density of the film is spatially controlled by using multiple UV illumination, which enables a controlled buckling of the film and forms various axisymmetric and non-axisymmetric structures [54]. A a similar approach was taken using grayscale photolithography (Fig. 6(j)) [55]. This shows a great potential to design programmed SCMs by controlling the internal stress of heterogeneously patterned structures.

4. Films with Internal Structures

Natural structures transform into complex 3-dimensional shapes using the mechanical stress of the organs. In particular, many plant organ systems have either bilayer structures [6,7] or fibrous internal structures [56,57]. These natural architectures offer efficient ways for the shape to change upon exposure to humidity, and provide a good inspiration for the material design. To mimic fibrous structures, anisotropic materials such as nanofibers or nanoplatelets have been engineered (Fig. 7(a)). Erb et al. incorporated aligned aluminum oxide (Al_2O_3) platelets to gelatin gels by applying a magnetic field [58]. To achieve this, the magnetic nanoparticles were

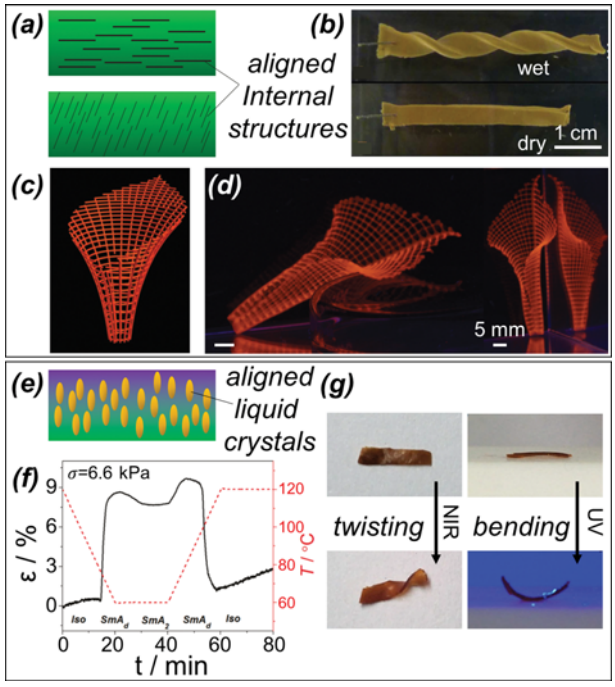

Fig. 7. (a) Schematic of SCMs with aligned internal structures. (b) Shape changing gelatin bilayers having aligned aluminum plates in 0 and $\pi/2$ angles, respectively, by applying magnetic field. The film remains flat at dried states (bottom) and forms twisted stated at fully hydrated states (top). Reproduced with permission [58]. Copyright 2013, Nature Publishing Group (c), (d) (c) Computer simulation and (d) experimental results for actuation of 3d printed hydrogels. Shape of materials after swelling is determined by overall architecture of materials as well as aligned cellulose within hydrogel scaffolds. Panel (c), (d) is reproduced with permission [52]. Copyright 2016, Nature Publishing Group. (e) Schematic of SCMs with aligned liquid crystals as an internal structure. (f) Change of strain responses of liquid crystalline terpolymer networks made of 5-{n-(cholesteryloxycarbonyl)-alkyloxycarbonyl}bicyclo[2.2.1]hept-2-ene, poly(ethylene glycol)-functionalized norbornene, and 5-(acryloyl butoxycarbonyl)bicyclo[2.2.1] hept-2-ene. As temperature varies (red), crystalline phases change among isotropic (iso), non-interdigitated bilayer (SmA_2), and interdigitated bilayer (SmA_d), repeatedly, and it results change of strain responses of film. Reproduced with permission [61]. Copyright 2011, American Chemical Society. (g) Light-driven actuation of liquid crystal soft actuator made of polymethylhydrosiloxane (PMHS)/(4-butoxy-phenyl)-(4-hex-5-enyloxy-phenyl)-diazene (AZO46)/4-pent-4-enyloxy-benzoic acid 4-butoxy-phenyl ester (MBB) composite and PMHS/MBB composite as a bilayer. For fabrication of bilayer, orientation of liquid crystals is prepared as 45 degree shifted between each other and NIR dye YHD796 is added for the actuation. The film is twisted under NIR light (left) and bended under UV light (right) due to the different liquid crystal orientation. Reproduced with permission [64]. Copyright 2016, Nature Publishing Group.

adsorbed on the Al_2O_3 platelets, and then an external magnetic field was applied prior to gelation. The hydration of monolithic gelatin-Al_2O_3 composite changes its shape using the direction-specific ori-

entation of the Al_2O_3, showing programmability (Fig. 7(b)). The carbon nanofibers are also used as fibrous materials with photothermal characteristics for programmable actuation [59]. Interestingly, 3D printing technology is used with fibrous materials to produce printable SCMs [52]. The shear forces generated by the hydrogel prepolymer flow from the deposition nozzle align cellulose fibrils parallel to the direction of flow, which determines the anisotropic elastic modulus of the final products. As a result, the curvature of the structures is precisely controlled and predicted, as shown in Figs. 7(c) and 7(d).

Liquid crystals are known to form various crystalline states with tunable optical properties. Of course, oriented liquid crystals shown in Fig. 7(e) have an effect on the mechanical properties and structure of the materials [60-62]. The SCMs with twisted and splayed liquid crystal structures have shown saddle-like, smooth structures, respectively, through the orientation of liquid crystals [60,62]. In addition, the reorientation of liquid crystals by the temperature also drives the change in the shape of the materials [61,63,64]. Ahn et al. used the reversible reorientation of the side-chain liquid crystalline polymer networks from smectic non-interdigitated to an interdigitated structure that can expand or contract materials with different strain responses (Fig. 7(f)). The bilayer liquid crystal elastomers with differently orientated liquid crystals show dual-responsive characteristic. Wang et al. bonded two liquid crystal elastomers with a 45° shifted angle to form a chiral structure, helix upon actuation [64]. In this strategy, each layer is designed to be actuated with different light sources, UV and NIR lights, showing dual responsive behaviors, as shown in Fig. 7(g).

5. Hinge and Patch Type Films

Inspired by traditional paper origami, active materials can be used as a hinge to produce an overall structure folded into 3-dimensional structures (Fig. 8(a)) [27,29,65-67]. Contrary to bilayer type materials, hinge type materials do not require bending or curling of their supporting materials since the active materials only connect separated supporting patches as a joint. Therefore, active materials are used to fold supporting patches as paper origami. The hinge-type folding mechanism enables the transformation of planar films into polyhedral structures. The early demonstration of hinge-type SCMs uses metal thin films [68,69], and photolithographic patterns of metal template with solder hinges are folded by melting the solder at high temperatures. Molten solders drive the folding of supporting patches resulting in various shape origami structures, and this is an irreversible process since the molten solder cannot be recovered into its original shape. The hinges made from polymeric materials broaden the types of stimuli that can be used for actuation. By using polymeric hinge-type SCMs, folding and unfolding have been demonstrated by melting, dissolution or degradation of the hinges; the Gracias group has reported various hinge-type SCMs. For example, polycaprolactone hinges are melted for surface tension-driven folding in the same way with the one made of solder (Fig. 8(b)) [70,71]. As a sacrificial domain, polymer hinges are also used to release the stress on pre-stressed planar films driving the folding of the materials. For stepwise folding and unfolding of the materials, Bassik et al. made two degradable biopolymer hinges on the metal thin film which can be applied as a microgripper [72]. The pre-stressed planar film is folded as a concave-down hinge that degrades by enzyme 1, and it is then unfolded as a concave-up hinge that degrades by enzyme 2, showing the gripping and release of the targets.

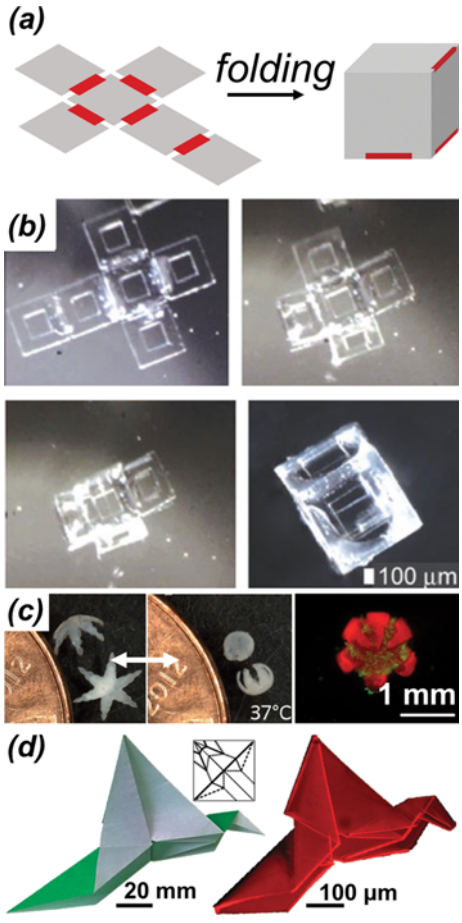

Fig. 8. (a) Illustration of hinge-assisted folding of SCMs. Active materials are patterned as hinge (red) and supporting materials are used as patches (gray). (b) Movie snapshots for irreversible self-folding of SU-8 polymer sheets as active hinges, polycaprolactone, is liquefied at 58 °C. Reproduced with permission [70]. Copyright 2011, Springer. (c) Temperature-responsive reversible folding (left, middle) of microgripper made of supporting patches, poly(propylene fumarate), active hinges of poly(N-isopropylacrylamide-co-acrylic acid). Deswelling of active hinges enable tight gripping of clump of cells (right). Reproduced with permission [66]. Copyright 2014, Wiley-VCH. (d) Origami inspired folding of poly(p-methylstyrene)/PNIPAM/poly(p-methylstyrene) trilayer film. Followed by traditional paper origami (left), supporting patches, poly(p-methylstyrne), are patterned for valley (inset, dotted line) and mountain (inset, solid line) at bottom and top of active layer, respectively, realizing the same self-folding structures (right). Reproduced with permission [73]. Copyright 2015, Wiley-VCH.

The stimuli-responsive hinges enable reversible folding of the materials, and the active hinges made of the PNIPAM-*co*-acrylic acid make the material temperature-responsive [66,67]. On the stiff polymer backbone, polypropylene fumarate, PNIPAM-*co*-acrylic acid is patterned as an active hinge. Hinge-type materials offer a mechanically strong microstructure in comparison with the bilayer

type of materials that require a soft supporting layer for transformation. As a result, folding the material provides sufficient force to grip the materials as well as to excise the cells that can be applied for biomedical and surgical applications, Fig. 8(c). The complexity of the shape change is enhanced when we carefully design the patterned structures. Literally speaking, complex origami folding is realized at a microscale by using stimuli-responsive polymers. Na et al. encoded a complex origami folding mechanism by introducing two patterned glassy polymers on the top and bottom sides of the PNIPAM film [73]. The direction of the folding and unfolding angles is pre-programmed in the glassy polymers by controlling the folding patterns and thickness of the film, respectively. This shows that the actuation of the SCMs can achieve multiple folding in series (Fig. 8(d)), and is very useful in addressing the fundamental problems of the folding mechanics and for applications as microrobotics and biomedical devices.

CONCLUDING REMARKS

Soft shape changing materials have been developed using a variety of materials and structures. Due to the technological advances in micropatterning, the design of the materials from micro- to nanoscale is no longer an issue. SCMs are now receiving a significant amount of attention not only from a biomedical, material, and chemical engineering standpoint but from mechanical engineering as soft robots. To meet such demands, the material properties and degree of freedom for actuation have to be improved. As far as the material properties are concerned, many studies have focused on showing bending, curling, or folding of materials to respond to external stimuli. The shape of the material before and after the actuation is too simple to produce complex robot-like structures. Moreover, the kinds of materials and actuation cues are quite limited with a few exceptions (Fig. 5), which should be further diversified in the future. In addition, mechanically robust materials are also required. In the case of the SCM made from hydrogels, the actuation and sample preparation should be performed carefully due to a poor mechanical strength. Recently, a double-network hydrogel that guarantees toughness as well as flexibility shows a bright side of hydrogels as an SCM [74]. The speed of actuation is another issue that can be improved by considering the actuation energy generated during the volume phase transition of the materials. Inspired by natural structures, such as Venus flytraps, rapid actuation, such as snapping, can be done by designing SCM to have a doubly-curved (e.g., hyperbolic) structure [7]. Most of all, the programmability of the material is of great importance for SCM. For multiple and orthogonal actuation of active layers, advanced actuation cues should be discovered. For example, DNA-responsive materials can be engineered into SCM with a number of orthogonal active layers thanks to the sequence-specific hybridization [38]. This may enable a multi-unit actuation system. In addition, temporally controlled actuation will provide sequential actuations to achieve the transformation of SCMs into multi-folded structures.

Although we did not cover it in this report, programmability can also be improved by adapting kirigami folding [75], and this idea has already been adapted demonstrating mechanically robust, highly stretchable, or optically anisotropic materials. Moreover, quite a few studies have reported the actuation of soft robots, such as walking [76], crawling [77], jumping [78] and so on, either using soft material only or combining it with electronic devices. These efforts will be combined with SCMs in the end, and the trend will continue considering the potential of soft SCMs, which will contribute to the design of various kinds of actuators and robots.

ACKNOWLEDGEMENT

This research was supported by Basic Science Research Program through the National Research Foundation of Korea (NRF) funded by the Ministry of Science, ICT & Future Planning (2016R1C1B2016089) and partially supported by the Ajou university research fund.

NOMENCLATURE

SCM : shape changing material
PAA : poly(acrylic acid)
PAH : poly(allyl-amine hydrochloride)
PNIPAM : poly(N-isopropylacrylamide)
LCST : lower critical solution temperature
p(HEMA) : poly(2-hydroxyethylmethacylate)
AA : acrylic acid
PEGDA : poly(ethylene glycol) diacrylate
BZ reaction : Belousov-Zhabotinsky reaction
T_{trans} : thermal transition temperature
Al_2O_3 : aluminum oxide
ABP : 4-acryloylbenzophenone
PAAm : poly(acrylamide)
GelMA : gelatin methacrylate
PEGDMA : polyethylene glycol dimethacrylate
PMHS : polymethylhydrosiloxane
AZO46 : (4-butoxy-phenyl)-(4-hex-5-enyloxy-phenyl)-diazene
MBB : 4-pent-4-enyloxy-benzoic acid 4-butoxy-phenyl ester
κ : curvature

REFERENCES

1. S.-K. Ahn, R. M. Kasi, S.-C. Kim, N. Sharma and Y. Zhou, *Soft Matter*, **4**, 1151 (2008).
2. I. Tokarev and S. Minko, *Soft Matter*, **5**, 511 (2009).
3. L. Ionov, *Langmuir*, **31**, 5015 (2015).
4. K. Oliver, A. Seddon and R. S. Trask, *J. Mater. Sci.*, **51**, 10663 (2016).
5. Y. Liu, J. Genzer and M. D. Dickey, *Prog. Polym. Sci.*, **52**, 79 (2016).
6. M. J. Harrington, K. Razghandi, F. Ditsch, L. Guiducci, M. Rueggeberg, J. W. C. Dunlop, P. Fratzl, C. Neinhuis and I. Burgert, *Nat. Commun.*, **2**, 337 (2011).
7. Y. Forterre, J. M. Skotheim, J. Dumais and L. Mahadevan, *Nature*, **433**, 421 (2005).
8. Y. Ma and J. Sun, *Chem. Mater.*, **21**, 898 (2009).
9. W. Li, G. Huang, H. Yan, J. Wang, Y. Yu, X. Hu, X. Wu and Y. Mei, *Soft Matter*, **8**, 7103 (2012).
10. J. Guan, H. He, D. J. Hansford and L. J. Lee, *J. Phys. Chem. B*, **109**, 23134 (2005).

11. Z. Hu, X. Zhang and Y. Li, *Science*, **269**, 525 (1995).
12. G. Stoychev, N. Puretskiy and L. Ionov, *Soft Matter*, **7**, 3277 (2011).
13. G. Stoychev, S. Zakharchenko, S. Turcaud, J. W. C. Dunlop and L. Ionov, *ACS Nano*, **6**, 3925 (2012).
14. A. W. Hauser, A. A. Evans, J.-H. Na and R. C. Hayward, *Angew. Chem. Int. Ed.*, **127**, 5524 (2015).
15. S. Fusco, M. S. Sakar, S. Kennedy and C. Peters, *Adv. Mater.*, **26**, 952 (2014).
16. E. Lee, D. Kim, H. Kim and J. Yoon, *Sci. Rep.*, **5**, 15124 (2015).
17. D. Kim, H. S. Lee and J. Yoon, *Sci. Rep.*, **6**, 5974 (2016).
18. L. Brannon-Peppas and N. A. Peppas, *Chem. Eng. Sci.*, **46**, 715 (1991).
19. T. S. Shim, S.-H. Kim, C.-J. Heo, H. C. Jeon and S.-M. Yang, *Angew. Chem. Int. Ed.*, **51**, 1420 (2012).
20. M. S. Oh, Y. S. Song, C. Kim, J. Kim, J. B. You, T.-S. Kim, C.-S. Lee and S. G. Im, *ACS Appl. Mater. Interfaces*, **8**, 8782 (2016).
21. P. Techawanitchai, M. Ebara, N. Idota, T.-A. Asoh, A. Kikuchi and T. Aoyagi, *Soft Matter*, **8**, 2844 (2012).
22. J. Duan, X. Liang, K. Zhu, J. Guo and L. Zhang, *Soft Matter*, **13**, 345 (2016).
23. S. Maeda, Y. Hara, T. Sakai, R. Yoshida and S. Hashimoto, *Adv. Mater.*, **19**, 3480 (2007).
24. E. Käpylä, S. M. Delgado and A. M. Kasko, *ACS Appl. Mater. Interfaces*, **8**, 17885 (2016).
25. J. C. Athas, C. P. Nguyen, B. C. Zarket, A. Gargava, Z. Nie and S. R. Raghavan, *ACS Appl. Mater. Interfaces*, **8**, 19066 (2016).
26. G. J. Berg, M. K. McBride, C. Wang and C. N. Bowman, *Polymer*, **55**, 5849 (2014).
27. Y. Liu, J. K. Boyles, J. Genzer and M. D. Dickey, *Soft Matter*, **8**, 1764 (2012).
28. H. Zhang, J. Zhang, X. Tong, D. Ma and Y. Zhao, *Macromol. Rapid Commun.*, **34**, 1575 (2013).
29. H. Zhang, H. Xia and Y. Zhao, *ACS Macro Lett.*, **3**, 940 (2014).
30. X. Xiao, D. Kong, X. Qiu, W. Zhang, F. Zhang, L. Liu, Y. Liu, S. Zhang, Y. Hu and J. Leng, *Macromolecules*, **48**, 3582 (2015).
31. M. Behl, K. Kratz, J. Zotzmann, U. Nöchel and A. Lendlein, *Adv. Mater.*, **25**, 4466 (2013).
32. A. Biswas, V. K. Aswal, P. U. Sastry, D. Rana and P. Maiti, *Macromolecules*, **49**, 4889 (2016).
33. R. R. Kohlmeyer, P. R. Buskohl, J. R. Deneault, M. F. Durstock, R. A. Vaia and J. Chen, *Adv. Mater.*, **26**, 8114 (2014).
34. S.-Q. Wang, D. Kaneko, M. Okajima, K. Yasaki, S. Tateyama and T. Kaneko, *Angew. Chem. Int. Ed.*, **52**, 11143 (2013).
35. X. Hu, J. Zhou, M. Vatankhah-Varnosfaderani, W. F. M. Daniel, Q. Li, A. P. Zhushma, A. V. Dobrynin and S. S. Sheiko, *Nat. Commun.*, **7**, 12919 (2016).
36. K. Kuribayashi-Shigetomi, H. Onoe and S. Takeuchi, *PLoS ONE*, **7**, e51085 (2012).
37. J. C. Nawroth, H. Lee, A. W. Feinberg, C. M. Ripplinger, M. L. McCain, A. Grosberg, J. O. Dabiri and K. K. Parker, *Nat. Biotechnol.*, **30**, 792 (2012).
38. T. S. Shim, Z. G. Estephan, Z. Qian, J. H. Prosser, S. Y. Lee, D. M. Chenoweth, D. Lee, S.-J. Park and J. C. Crocker, *Nat. Nanotech.*, **12**, 41 (2016).
39. C. Ye, S. V. Nikolov, R. D. Geryak, R. Calabrese, J. F. Ankner, A. Alexeev, D. L. Kaplan and V. V. Tsukruk, *ACS Appl. Mater. Interfaces*, **8**, 17694 (2016).
40. G. Stoychev, L. Guiducci, S. Turcaud, J. W. C. Dunlop and L. Ionov, *Adv. Funct. Mater.*, **26**, 7733 (2016).
41. T.-A. Asoh, M. Matsusaki, T. Kaneko and M. Akashi, *Adv. Mater.*, **20**, 2080 (2008).
42. Y. Zhang and L. Ionov, *ACS Appl. Mater. Interfaces*, **6**, 10072 (2014).
43. R. Luo, J. Wu, N.-D. Dinh and C.-H. Chen, *Adv. Funct. Mater.*, **25**, 7272 (2015).
44. Y. Zhang and L. Ionov, *Langmuir*, **31**, 4552 (2015).
45. Y. Liao, N. An, N. Wang, Y. Zhang, J. Song, J. Zhou and W. Liu, *Macromol. Rapid Commun.*, **36**, 2129 (2015).
46. H. Thelén-Aubin, M. Moshe, E. Sharon and E. Kumacheva, *Soft Matter*, **11**, 4600 (2015).
47. C. Ma, X. Le, X. Tang, J. He, P. Xiao, J. Zheng, H. Xiao, W. Lu, J. Zhang, Y. Huang and T. Chen, *Adv. Funct. Mater.*, **26**, 8670 (2016).
48. Z. J. Wang, C. N. Zhu, W. Hong, Z. L. Wu and Q. Zheng, *J. Mater. Chem. B*, **4**, 7075 (2016).
49. H. Thérien-Aubin, Z. L. Wu, Z. Nie and E. Kumacheva, *J. Am. Chem. Soc.*, **135**, 4834 (2013).
50. Z. Wei, Z. Jia, J. Athas, C. Wang, S. R. Raghavan, T. Li and Z. Nie, *Soft Matter*, **10**, 8157 (2014).
51. P. Chen, S. He, Y. Xu, X. Sun and H. Peng, *Adv. Mater.*, **27**, 4982 (2015).
52. A. Sydney Gladman, E. A. Matsumoto, R. G. Nuzzo, L. Mahadevan and J. A. Lewis, *Nat. Mater.*, **15**, 413 (2016).
53. J. Kim, J. A. Hanna, R. C. Hayward and C. D. Santangelo, *Soft Matter*, **8**, 2375 (2012).
54. J. Kim, J. A. Hanna, M. Byun, C. D. Santangelo and R. C. Hayward, *Science*, **335**, 1201 (2012).
55. J.-H. Na, N. P. Bende, J. Bae, C. D. Santangelo and R. C. Hayward, *Soft Matter*, **12**, 4985 (2016).
56. C. Dawson, J. Vincent and A. M. Rocca, *Nature*, **390**, 668 (1997).
57. R. Elbaum, L. Zaltzman, I. Burgert and P. Fratzl, *Science*, **316**, 884 (2007).
58. R. M. Erb, J. S. Sander, R. Grisch and A. R. Studart, *Nat. Commun.*, **4**, 1712 (2013).
59. J. Deng, J. Li, P. Chen, X. Fang, X. Sun, Y. Jiang, W. Weng, B. Wang and H. Peng, *J. Am. Chem. Soc.*, **138**, 225 (2016).
60. G. N. Mol, K. D. Harris, C. W. M. Bastiaansen and D. J. Broer, *Adv. Funct. Mater.*, **15**, 1155 (2005).
61. S.-K. Ahn, P. Deshmukh, M. Gopinadhan, C. O. Osuji and R. M. Kasi, *ACS Nano*, **5**, 3085 (2011).
62. R. S. Kularatne, H. Kim, M. Ammanamanchi, H. N. Hayenga and T. H. Ware, *Chem. Mater.*, **28**, 8489 (2016).
63. A. W. Hauser, D. Liu, K. C. Bryson, R. C. Hayward and D. J. Broer, *Macromolecules*, **49**, 1575 (2016).
64. M. Wang, B.-P. Lin and H. Yang, *Nat. Commun.*, **7**, 1 (2016).
65. K.-U. Jeong, J.-H. Jang, D.-Y. Kim, C. Nah, J. H. Lee, M.-H. Lee, H.-J. Sun, C.-L. Wang, S. Z. D. Cheng and E. L. Thomas, *J. Mater. Chem.*, **21**, 6824 (2011).
66. K. Malachowski, J. Breger, H. R. Kwag, M. O. Wang, J. P. Fisher, F. M. Selaru and D. H. Gracias, *Angew. Chem. Int. Ed.*, **53**, 8045 (2014).
67. J. C. Breger, C. Yoon, R. Xiao, H. R. Kwag, M. O. Wang, J. P. Fisher, T. D. Nguyen and D. H. Gracias, *ACS Appl. Mater. Interfaces*, **7**, 3398 (2015).

68. E. Smela, O. Inganäs and I. Lundström, *Science*, **268**, 1735 (1995).
69. T. Leong, Z. Gu, T. Koh and D. H. Gracias, *J. Am. Chem. Soc.*, **128**, 11336 (2006).
70. A. Azam, K. E. Laflin, M. Jamal, R. Fernandes and D. H. Gracias, *Biomed. Microdevices*, **13**, 51 (2011).
71. J. S. Randhawa, T. G. Leong, N. Bassik, B. R. Benson, M. T. Jochmans and D. H. Gracias, *J. Am. Chem. Soc.*, **130**, 17238 (2008).
72. N. Bassik, A. Brafman, A. M. Zarafshar, M. Jamal, D. Luvsanjav, F. M. Selaru and D. H. Gracias, *J. Am. Chem. Soc.*, **132**, 16314 (2010).
73. J.-H. Na, A. A. Evans, J. Bae, M. C. Chiappelli, C. D. Santangelo, R. J. Lang, T. C. Hull and R. C. Hayward, *Adv. Mater.*, **27**, 79 (2015).
74. J.-Y. Sun, X. Zhao, W. R. K. Illeperuma, O. Chaudhuri, K. H. Oh, D. J. Mooney, J. J. Vlassak and Z. Suo, *Nature*, **489**, 133 (2012).
75. T. C. Shyu, P. F. Damasceno, P. M. Dodd, A. Lamoureux, L. Xu, M. Shlian, M. Shtein, S. C. Glotzer and N. A. Kotov, *Nat. Mater.*, **14**, 785 (2015).
76. M. T. Tolley, R. F. Shepherd, B. Mosadegh, K. C. Galloway, M. Wehner, M. Karpelson, R. J. Wood and G. M. Whitesides, *Soft Robotics*, **1**, 213 (2014).
77. M. Rogóż, H. Zeng, C. Xuan, D. S. Wiersma and P. Wasylczyk, *Adv. Opt. Mater*, **4**, 1689 (2016).
78. N. W. Bartlett, M. T. Tolley, J. T. B. Overvelde, J. C. Weaver, B. Mosadegh, K. Bertoldi, G. M. Whitesides and R. J. Wood, *Science*, **349**, 161 (2015).

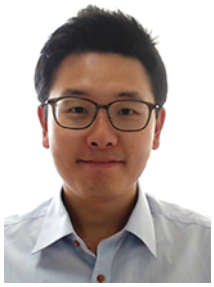

Tae Soup Shim is an assistant professor in Department of Chemical Engineering and Department of Energy Systems Research, Ajou University, Korea. He received his BS degree in Chemical Engineering from Yonsei University, Korea, in 2007 and a PhD degree in Chemical and Biomolecular Engineering from KAIST, Korea, in 2013 under the supervision of the late Prof. Seung-Man Yang. Following this, he worked as a postdoctoral researcher at Department of Chemical and Biomolecular Engineering, University of Pennsylvania, USA. His major research interests include colloidal self-assembly, stimuli-responsive materials, interfacial phenomena, and biomimetics.